

Published in final edited form as:

Neuron. 2013 October 2; 80(1): 64–71. doi:10.1016/j.neuron.2013.07.014.

Accelerated Experience-dependent Pruning of Cortical Synapses in *Ephrin-A2* Knockout Mice

Xinzhu Yu¹, Gordon Wang², Anthony Gilmore¹, Ada Xin Yee³, Xiang Li⁴, Tonghui Xu¹, Stephen J Smith², Lu Chen³, and Yi Zuo^{1,*}

¹Department of Molecular Cell and Developmental Biology, University of California, Santa Cruz, Santa Cruz, CA 95064, USA.

²Department of Molecular and Cellular Physiology, Stanford University, Stanford, CA 94305, USA.

³Department of Psychiatry and Behavioral Science, Stanford University, Stanford, CA 94305, USA.

⁴Department of Neuroscience, Columbia University, New York, NY 10032, USA.

SUMMARY

Refinement of mammalian neural circuits involves substantial experience-dependent synapse elimination. Using *in vivo* two-photon imaging, we found that experience-dependent elimination of postsynaptic dendritic spines in the cortex was accelerated in *ephrin-A2* knockout (KO) mice, resulting in fewer adolescent spines integrated into adult circuits. Such increased spine removal in *ephrin-A2* KOs depended on activation of glutamate receptors, as blockade of the *N*-methyl-D-aspartate (NMDA) receptors eliminated the difference in spine loss between wild-type and KO mice. We also showed that ephrin-A2 in the cortex colocalized with glial glutamate transporters, which were significantly down-regulated in *ephrin-A2* KOs. Consistently, glial glutamate transport was reduced in *ephrin-A2* KOs, resulting in an accumulation of synaptic glutamate. Finally, inhibition of glial glutamate uptake promoted spine elimination in wild-type mice, resembling the phenotype of *ephrin-A2* KOs. Together, our results suggest that ephrin-A2 regulates experience-dependent, NMDA receptor-mediated synaptic pruning through glial glutamate transport during maturation of the mouse cortex.

INTRODUCTION

Postnatal experience-dependent synapse elimination is crucial for the establishment of properly connected neuronal circuits in the mature brain. Synapse elimination prunes the supernumerary imprecise connections formed during the initial overproduction of synapses, while strengthening functionally important connections (Changeux and Danchin, 1976; Hubel et al., 1977; Katz and Shatz, 1996; Lichtman and Colman, 2000). The majority of excitatory glutamatergic synapses in the mammalian brain reside at dendritic spines, which contain all necessary postsynaptic signaling machinery and serve as a good proxy for synaptic connectivity (Nimchinsky et al., 2002; Segal, 2005; Tada and Sheng, 2006; Yuste

© 2013 Elsevier Inc. All rights reserved.

*To whom correspondence should be addressed. yizuo@ucsc.edu.

Publisher's Disclaimer: This is a PDF file of an unedited manuscript that has been accepted for publication. As a service to our customers we are providing this early version of the manuscript. The manuscript will undergo copyediting, typesetting, and review of the resulting proof before it is published in its final citable form. Please note that during the production process errors may be discovered which could affect the content, and all legal disclaimers that apply to the journal pertain.

and Bonhoeffer, 2001). Recent *in vivo* two-photon imaging studies have shown that dendritic spines of cortical pyramidal neurons across various cortical regions undergo rapid elimination during adolescent development. In the adult brain, spine elimination continues at a much lower rate, and spines surviving the pruning process build the foundation of the mature circuits (Holtmaat et al., 2005; Yang et al., 2009; Zuo et al., 2005a; Zuo et al., 2005b). Although experience or activity-dependent plasticity is believed to drive the extensive and prolonged synaptic pruning, the molecular mechanisms underlying this process remain largely unknown.

Ephrins and their Eph receptors are attractive candidates for modulating structural plasticity of synapses, because of their synaptic expression and ability to coordinate contact-mediated bidirectional signaling in ligand- and receptor-containing cells (Aoto and Chen, 2007; Klein, 2009; Lai and Ip, 2009; Murai and Pasquale, 2004). Based on their cell membrane attachment and binding preference to Eph receptors, ephrins are classified into two groups: 1) GPI-linked ephrin-As that preferentially interact with EphA receptors and 2) transmembrane ephrin-Bs that preferentially bind to EphB receptors. While it is generally believed that ephrin-Bs and EphB receptors act through trans-synaptic interactions to modulate synapse development and plasticity, ephrin-As and EphA receptors have been shown to mediate astrocyte-neuron interactions at mature hippocampal synapses. In particular, ephrin-A3 ligands are expressed in astrocytic processes, and EphA4 receptors are localized to postsynaptic spines of CA1 pyramidal neurons (Murai et al., 2003). In cultured hippocampal slices, while activation of EphA4 receptors by ephrin-A3 ligands induces spine retraction, disruption of this interaction leads to elongation of spine length (Murai et al., 2003). However, the roles of ephrin-As in experience-dependent synaptic pruning remain unknown.

In this study, we show that elimination of dendritic spines from cortical pyramidal neurons is greatly enhanced in *ephrin-A2*, but not *ephrin-A3*, KO mice during adolescent development, through an experience-dependent, NMDA receptor-mediated mechanism. The imbalance between spine formation and elimination leads to an accelerated reduction in the number of total spines in adult mice. We also find that glial glutamate transporters (GLAST and GLT-1) are closely associated with ephrin-A2 proteins. The expression of glial glutamate transporters is down-regulated in *ephrin-A2* KOs, resulting in decreased glial glutamate uptake and increased synaptic glutamate level. Finally, pharmacological inhibition of glial glutamate uptake promotes spine elimination in the cortex of wild-type mice.

RESULTS

***Ephrin-A2* KO Mice Have Elevated Spine Elimination in the Cortex during Adolescent Development**

To investigate whether and how ephrin-As affect synapse development, we crossed *ephrin-A2* or *ephrin-A3* single and double KO mice with YFP-H line mice, which express cytoplasmic yellow fluorescent protein (YFP) predominantly in a subpopulation of layer V cortical neurons (Feng et al., 2000). We did not find any difference in cortical organizations or spine density along apical dendrites in layer V neurons between *ephrin-A2/A3* KO and wild-type mice at one month of age (Figure S1). To determine if spine dynamics were affected in *ephrin-A* KOs, we repeatedly imaged apical dendritic branches and followed spine dynamics in the motor cortex by transcranial two-photon microscopy. We found that, while the amount of new spines added over 2 days was comparable between *ephrin-A2* KOs and their wild-type littermates, significantly more spines were eliminated during the same period of time in KOs (Figures 1A, 1B and 1E; $P < 0.001$). Unlike *ephrin-A2* KOs, *ephrin-A3* KOs exhibited similar spine turnover to wild-type controls (Figures 1C and 1E; $P > 0.1$). In addition, spine elimination in *ephrin-A2/A3* double KOs was comparable to that of *ephrin-*

A2 single KOs (Figures 1D and 1E; $P>0.7$). Moreover, we found that the increase in spine elimination occurred in various cortical regions of *ephrin-A2* KOs (Figure S2), and persisted over prolonged imaging intervals (Figure 1F). As a consequence, despite the normal spine density at one month of age ($P>0.2$), spine density of adult *ephrin-A2* KOs was lower than that of wild-type mice (Figure 1G; $P<0.05$). Thus, developmentally-regulated spine pruning is accelerated in *ephrin-A2* KOs.

Fewer Adolescent Spines Are Incorporated into the Adult Neural Circuits in *Ephrin-A2* KO Mice

Spines formed during early development and surviving extensive pruning have greatly contributed to stably connected neural networks in adulthood (Yang et al., 2009; Zuo et al., 2005a). To investigate how accelerated spine elimination during adolescent development influences adult synaptic connections in *ephrin-A2* KOs, we calculated the lifetime of dendritic spines in both wild-type and *ephrin-A2* KO mice, based on spine elimination measured over various imaging intervals (*i.e.*, 2, 4, 8, 30 and 90 days), starting at one month of age (Figure 1F). We found that the spine survival curve of wild-type mice was well fitted by a two-phase exponential decay equation ($R^2=0.92$, see Experimental Procedures), with a small portion of spines rapidly lost (“fast-decay spines”, 15%, half-life 3.0 days) and the rest stable over months (“slow-decay spines”, half-life 1112 days). Fitting the spine survival curve of *ephrin-A2* KOs with the same formula ($R^2=0.90$), we found that while the half-life of the fast-decay spine population in KOs was comparable to that of wild-type mice (2.3 days, $P>0.4$), the half-life of the slow-decay spine population was significantly shorter in KOs (432 days, $P<0.01$). As previous studies have revealed that newly formed spines are much more vulnerable to elimination than pre-existing spines (Xu et al., 2009; Yang et al., 2009), the fast- and slow-decay spines could represent new and pre-existing spines, respectively. To determine if the survival of new and pre-existing spines was, indeed, affected differently in *ephrin-A2* KOs, we imaged the same mice 3 times (*i.e.* day 0, 1 and 5), identified new spines and pre-existing spines based on their appearance in the first two images, and quantified their survival rates using the last images. Indeed, while the survival rate of new spines was comparable between *ephrin-A2* KO and wild-type mice ($P>0.5$), the survival rate of pre-existing spines was significantly lower in *ephrin-A2* KOs (Figure 1H; $P<0.05$). Such results agree with the lifetime analysis, suggesting a selective, but long-lasting effect of *ephrin-A2* on the removal of stable spines.

Sensory Experience Is Required for Elevated Spine Elimination in the Barrel Cortex of Adolescent *Ephrin-A2* KO Mice

Experience drives synapse elimination during postnatal development. We found that deprivation of sensory experience by unilateral whisker trimming at one month of age significantly reduced spine elimination in the contralateral barrel cortex of both wild-type and *ephrin-A2* KO mice (Figures 2A–2D and 2G; $P<0.005$). In contrast, spine formation was unaffected by whisker trimming over the same period (Figure S3). Furthermore, there was no difference in spine elimination between deprived wild-type and deprived KO mice ($P>0.2$), suggesting that sensory experience is necessary for elevated spine elimination in *ephrin-A2* KOs.

In contrast to sensory deprivation, different environmental enrichment (EE) protocols have been shown to promote both spine elimination and spine formation in various cortical areas of living mice (Fu et al., 2012; Yang et al., 2009). Using a sensory EE paradigm, we found that spine elimination in the barrel, but not the motor, cortex of both wild-type and KO mice was robustly increased, and significantly more spines were removed in KOs compared with wild-type mice under sensory EE (Figures 2E–2G and S3; $P<0.005$). In addition, sensory EE promoted spine formation to comparable high levels in wild-type and KO mice (Figure S3).

Together, these results indicate that lack of ephrin-A2 selectively affects experience-dependent spine loss, but not experience-dependent spine growth.

NMDA Receptors Mediate Elevated Spine Elimination in *Ephrin-A2* KO Mice

Many lines of evidence have shown that NMDA receptor activation is essential for synaptic plasticity in various systems (Bock and Braun, 1999; Nicoll and Malenka, 1999; Sawtell et al., 2003; Sin et al., 2002). We found that, in the barrel cortex, blockade of NMDA receptors affected spine elimination in a fashion similar to that of sensory deprivation. Four-day treatment with MK801, a selective antagonist of NMDA receptors, significantly decreased spine elimination in both wild-type and *ephrin-A2* KO mice (Figure 2G; $P < 0.05$), without affecting spine formation (Figure S3). MK801 treatment also eliminated the differences in spine loss between wild-type and KO mice ($P > 0.7$), suggesting that elevated spine elimination in *ephrin-A2* KOs is mediated by NMDA receptors.

Ephrin-A2 Colocalizes with Glial Glutamate Transporters in the Mouse Cortex

The expression of both ephrin-A2 and ephrin-A3 mRNAs in embryonic and adult mouse cortices is well documented (Cang et al., 2005; Murai et al., 2003; Torii et al., 2009). A transcriptome database has reported cell-type-specific expression profiles of ephrin-A2 and ephrin-A3 in the mouse forebrain: while ephrin-A2 mRNAs are enriched in astrocytes, ephrin-A3 mRNAs are enriched in neurons (Cahoy et al., 2008). However, little is known about the cortical expression of their protein products. To address this question, we took advantage of array tomography (AT), a proteomic imaging method that offers the ability to resolve individual synapses and analyze their protein profiles at ultrastructural level (Micheva et al., 2010; Micheva and Smith, 2007). As illustrated in Figures 3A and 3B, individual ephrin-A2 and ephrin-A3 puncta were clearly resolved using AT from cortical sections of adolescent wild-type mice, but not *ephrin-A2/A3* KOs (Figure S4). The densities of ephrin-A2 and ephrin-A3 puncta were relatively consistent throughout all cortical layers (Figure S4). Subsequent quantitative analyses further revealed that the density of ephrin-A2 puncta was approximately 3 times the density of ephrin-A3 puncta in the superficial cortical layers (Figure 3C).

To further investigate the subcellular localizations of ephrin-As near cortical synapses, we co-labeled ephrin-A2 and ephrin-A3 proteins with different synaptic (presynaptic: bassoon, synapsin, VGluT1 and SV2; postsynaptic: PSD95) and astrocytic (GLAST, GLT-1 and GS) markers (Figures 3D and 3E), and then analyzed the spatial distribution of ephrin-As around different protein constituents in three dimensions at excitatory synapses. Our analyses revealed that the numbers of ephrin-A2 puncta within 100 nm from the centers of astrocytic proteins, especially GLAST and GLT-1, were higher than those around neuronal synaptic markers (Figure 3F), whereas ephrin-A3 puncta were more aligned to presynaptic markers (Figure S4). Membrane-bound glial glutamate transporters, GLAST and GLT-1, are enriched in perisynaptic astrocytic processes and associated tightly with excitatory synapses (Chaudhry et al., 1995). Thus, in agreement with the transcriptome data, our results show that while ephrin-A3 is predominantly presynaptic, ephrin-A2 localizes predominantly to astrocytic processes near synapses.

Glial Glutamate Transporters Are Down-regulated in *Ephrin-A2* KO Mice

Having shown that ephrin-A2 colocalized with glial glutamate transporters, we next examined if cortical expression of glial glutamate transporters was altered in *ephrin-A2* KOs. While the density, size and morphology of cortical astrocytes were indistinguishable between wild-type and *ephrin-A2* KO mice (Figure S5), cortical expression levels of GLAST and GLT-1 were significantly decreased compared with wild-type controls (Figures 4A, 4B and S5). Specifically, there was about 25% reduction of GLAST ($P < 0.05$) and about

40% reduction of GLT-1 ($P < 0.05$) in *ephrin-A2* KOs. In contrast, the expression of GS, another astrocytic enzyme involved in glutamate recycling (Hertz and Zielke, 2004), remained unaltered in *ephrin-A2* KOs (Figures 4A and 4B; $P > 0.4$). Further analysis of mRNA expression of GLAST and GLT-1 revealed a comparable level between wild-type and *ephrin-A2* KO mice (Figure S5), suggesting that down-regulation of GLAST and GLT-1 occurs at the posttranscriptional level in *ephrin-A2* KOs. Moreover, a decreasing trend in the expression of glial glutamate transporters was found in the contralateral barrel cortex following whisker trimming in both wild-type and KO mice (Figure S5), indicating an experience-dependent modulation of glial glutamate uptake.

Glial Glutamate Transport Is Reduced and Synaptic Glutamate Level Is Elevated in *Ephrin-A2* KO Mice

Membrane-bound glial glutamate transporters uptake glutamate from the synaptic cleft to regulate synaptic transmission (Tzingounis and Wadiche, 2007). We next investigated whether glutamate transport was affected in *ephrin-A2* KO mice, using radioactive tracer L -[3 H]-glutamate on cortical slices of one-month-old mice. We found that the efficiency of glutamate uptake was reduced by about 17% in *ephrin-A2* KOs compared with wild-type mice (Figure 4C; $P < 0.05$). Moreover, in the presence of high-affinity blocker of glial glutamate transporters, (3*S*)-3-[[3-[[4-(trifluoromethyl)benzoyl]amino]phenyl]methoxy]-*L*-aspartic acid (TFB-TBOA), glutamate uptake was decreased to comparable low levels in wild-type and KO cortical slices (Figure 4C), suggesting that reduced glutamate uptake is mostly due to decreased functions of glial glutamate transporters in *ephrin-A2* KOs. In addition, we found that dihydrokainate (DHK), a selective GLT-1 inhibitor, reduced glutamate uptake by $17.6 \pm 2.4\%$ in wild-type slices and $10.1 \pm 4.4\%$ in KO slices (Figure 4C). This result corresponded to an approximate 50% less DHK-sensitive uptake in KO slices.

Reduction in glial glutamate transporters has been previously demonstrated to result in an accumulation of extracellular glutamate both *in vivo* and *in vitro* (Rothstein et al., 1996). To assess synaptic glutamate concentrations, we performed whole-cell patch-clamp recordings from layer V pyramidal neurons in cortical slices of one-month-old mice and tested the sensitivity of the eEPSCs to L -2-amino-5 phosphonovalerate (L -APV), a low-affinity NMDA receptor antagonist with a fast off-rate. The degree of inhibition by L -APV inversely correlates with synaptic glutamate level (*e.g.* less inhibition by L -APV indicates higher synaptic glutamate concentration) (Choi et al., 2000). We found that the eEPSCs from KO slices were much less sensitive to L -APV (reduced by $31.9 \pm 7.1\%$) than those recorded from wild-type slices (reduced by $58.7 \pm 6.3\%$) (Figure 4D; $P < 0.05$), indicative of an elevated synaptic glutamate level in KO mice, possibly caused by reduced glial glutamate transport into astrocytes.

Reduction in Glial Glutamate Transport Promotes Spine Elimination

To further investigate the correlation between reduced glial glutamate transport and promoted spine removal *in vivo*, we treated wild-type mice with DHK, which is permeable to the blood brain barrier, and followed spine turnover. We found that spine elimination, but not formation, was significantly increased in one-month old wild-type mice treated with DHK for 4 days (Figure 4E), a phenotype that resembles the elevated spine loss in *ephrin-A2* KOs. This result suggests that normal glial uptake of glutamate is necessary for maintaining the stability of dendritic spines in the adolescent mouse cortex.

DISCUSSION

During early development, generation of excessive synapses occurs in a constitutive, genetically programmed manner. This initial overproduction of synapses is followed by an

experience-dependent pruning process that reduces synaptic connections considerably and leads to maturation of refined neural circuits. While experience is generally believed to be crucial for synapse elimination at this stage, little is known about its underlying molecular mechanisms. In this study, we identify ephrin-A2 as a participant in experience-dependent pruning of cortical synapses. Deficiency of ephrin-A2 selectively promotes experience-induced removal of existing spines, without affecting spine formation or initial stabilization. We further show that ephrin-A2 colocalizes with glial glutamate transporters and regulates synaptic glutamate transmission, suggesting a potential contribution of astrocytes to synaptic pruning during adolescent development.

To date, little is known about the downstream mechanisms of ephrin-A2 regulation of glial glutamate transporters. Ephrin-A2 may be involved in stabilizing glial glutamate transporters at cell membrane by preventing internalization and subsequent degradation. The fact that ephrin-As only contain a GPI-linked domain to anchor them to the membrane makes them depend on other proteins to transduce intracellular signals. Src family protein kinases have been identified as important signaling intermediates downstream of ephrin-As (Davy et al., 1999; Huai and Drescher, 2001; Zimmer et al., 2007). Furthermore, it has been demonstrated that Src kinases participate in regulating expression and maintaining functions of glial glutamate transporters (Koeberle and Bahr, 2008; Rose et al., 2009). The colocalization of ephrin-A2 and glial glutamate transporters also suggests a potential functional crosstalk between ephrin-A2 and glial glutamate transporters that relies on their physical proximity. However, how ephrin-A2 modulates glial glutamate transporters at perisynaptic astrocytic processes needs to be further investigated.

Glutamate transmission and activation of NMDA receptors are involved in both activity-dependent competition and homeostatic regulations – two fundamental mechanisms underlying synaptic plasticity. A critical task of astrocytes in the brain is to remove excess glutamate from the synaptic cleft, thereby ensuring precise synaptic transmission and preventing overactivation of postsynaptic glutamate receptors (Tzingounis and Wadiche, 2007). Thus, reduced glial glutamate uptake in *ephrin-A2* KOs presumably prolongs the effect of synaptic glutamate on postsynaptic NMDA receptors. Enhanced glutamate signaling at active synapses would subsequently augment the imbalance between activate and inactivate synapses, promoting competition-dependent spine elimination via a Hebbian mechanism. Alternatively, a global overactivation of postsynaptic glutamate receptors could trigger homeostatic regulation and lead to a reduction in total synapse number. It is also possible that a combination of these mechanisms contributes to increased spine loss in *ephrin-A2* KOs.

Previous studies have shown that ephrin-A3 is the most abundant ephrin-A ligand in the adult hippocampus and is involved in the morphogenesis of dendritic spines on CA1 pyramidal neurons (Carmona et al., 2009; Murai et al., 2003). Here, we show that ephrin-A2 is more predominant than ephrin-A3 in the cortex and that lack of ephrin-A2, but not ephrin-A3, results in accelerated experience-dependent spine pruning in the adolescent cortex. Moreover, while glial glutamate transporters are up-regulated in the hippocampus of *ephrin-A3* KOs (Carmona et al., 2009; Filosa et al., 2009), they are significantly down-regulated in the cortex of *ephrin-A2* KOs. Therefore, despite the fact that multiple ephrin-As are functionally redundant in topographic map formation and cortical column integration during early development (Cang et al., 2005; Cutforth et al., 2003; Feldheim et al., 2000; Pfeiffenberger et al., 2005; Torii et al., 2009), our findings suggest that different ephrin-As may regulate synapse morphology and dynamics through distinctive cellular signaling, providing a potential mechanism for achieving the specificity and complexity of mature neuronal networks.

EXPERIMENTAL PROCEDURES

Animals

Thy1-YFP-H line mice (Feng et al., 2000) were purchased from Jackson Laboratory. *Ephrin-A2* and *ephrin-A3* KO mice (Cutforth et al., 2003; Feldheim et al., 2000) were obtained from Dr. David A. Feldheim at UCSC. Wild-type littermates were used as controls and no difference in all analyses was observed between wild-type and heterozygous mice. Sensory deprivation was performed by cutting the mystacial vibrissae of the one side whisker-pad to skin level. Sensory enrichment was conducted by housing mice in a standard cage with about 180 strings of beads hanging from the top of the cage, with the string locations changed daily. MK801 (0.25 $\mu\text{g/g}$ body weight) and DHK (10 $\mu\text{g/g}$ body weight) were intraperitoneally injected. Mice were housed and bred in UCSC animal facilities according to approved animal protocol.

In Vivo Transcranial Imaging and Data Quantification

The surgical procedure for transcranial two-photon imaging and data quantification have been described previously (Xu et al., 2009). Percentages of eliminated and formed spines were normalized to total spines counted in the initial image. Spine density was calculated by dividing the number of spines by the length of the dendritic segment. For the spine lifetime analysis, data were fitted with a two-exponential-decay equation using GraphPad Prism: percentage of survival spine = $p_1 \times (1/2)^{t/\tau_1} + p_2 \times (1/2)^{t/\tau_2}$ (p_1 and p_2 : proportion of fast- and slow-decay spines, $p_1 + p_2 = 100\%$; τ_1 and τ_2 : half-life of fast- and slow-decay spines).

Array Tomography and Data Quantification

Array tomography experiments were performed as previously described (Micheva and Smith, 2007). Briefly, the mouse brain was dissected, fixed, dehydrated and embedded in London Resin (LR) White. Serial 70 nm sections were obtained and then probed consecutively with the following primary antibodies: mouse anti-bassoon (1:100; Abcam), mouse anti-SV2 (1:100; DSHB), rabbit anti-synapsin (1:100; Cell Signaling Technology), guinea pig anti-VGluT1 (1:100; Millipore), rabbit anti-PSD95 (1:100; Cell Signaling Technology), mouse-anti-NR1 (1:100; Millipore), mouse anti-GluR2 (1:100; Millipore), rabbit anti-GLAST (1:100), rabbit anti-GLT-1 (1:100), mouse anti-GS (1:100; BD Biosciences), rabbit anti-ephrin-A2 (1:100; Santa Cruz Biotechnology) and goat anti-ephrin-A3 (1:100; Invitrogen). All images were obtained using a Zeiss Axio Imager.Z1 Upright Fluorescence Microscope with motorized stage and Axiocam HR Digital Camera. Image data from sequential sections were computationally aligned, registered and unwarped. The density of ephrin-As puncta was calculated by dividing puncta numbers by the imaged volume subtracted by the volume of the nuclei. For colocalization analysis, the center of each protein punctum was identified and excitatory synapses were defined using PSD95, SV2 and VGluT1 puncta. Relative distances of ephrin-As centers to other neuronal and astrocytic protein centers within 1 μm from the centers of defined synapses were measured in three dimensions. The numbers of ephrin-As puncta within 100 nm from different protein centers were counted and normalized by total numbers of each protein centers.

Western Blots and Data Quantification

Cortical tissues were dissected and homogenized in ice-cold buffer solution. Denatured lysates were electrophoretically separated by 10% SDS-PAGE and transferred onto nitrocellulose membrane. This was then probed with primary antibodies against GLAST, GLT-1, GS, actin and tubulin. Western blots were quantified using ImageJ software. Detailed procedures are provided in Supplemental Information.

Glutamate Uptake Assay

Mice (P28–P30) were decapitated and cortical slices (400 μm thick) were prepared in cold artificial cerebrospinal fluid (ACSF) and maintained at room temperature for 1.5–2 h before stimulation. Cortical slices were incubated for 7 min in ACSF containing 0.5 μCi L -[^3H]-glutamate and 100 μM unlabeled glutamate and then rinsed with cold ACSF and homogenized in 1% Triton buffer. The radioactivity of 25 μl lysates was measured and glutamate uptake was normalized to protein concentration. To inhibit glial glutamate transporter-mediated uptake, cortical slices were incubated with 300 μM TFB-TBOA or 500 μM DHK for 30 min prior to uptake measurement.

Cortical Slice Electrophysiology

Coronal slices of the somatosensory cortex were prepared from mice (P28–P30) in ice cold cutting solution, and incubated in ACSF for 30 min at 32°C and 1 h at room temperature before recording. Whole-cell recordings were made from layer V pyramidal neurons. Synaptic currents were evoked at 0.05 Hz using a concentric bipolar stimulating electrode placed in layer II/III of the same whisker-barrel column. To isolate NMDA receptor currents, cells were voltage-clamped at -70 mV and perfused with an extracellular recording solution lacking Mg^{2+} , in the presence of 10 μM CNQX and 100 μM picrotoxin. To assess concentration of cleft-glutamate, 250 μM L -APV was bath-applied in the same Mg^{2+} -lacking solution with 10 μM CNQX and 100 μM picrotoxin. Analysis was done using ClampFit. Detailed procedures are provided in Supplemental Information.

Statistics

P-values were calculated using the Student's *t*-test. The numbers of cells/mice analyzed were indicated in the figure.

Supplementary Material

Refer to Web version on PubMed Central for supplementary material.

Acknowledgments

We gratefully thank David Feldheim for providing *ephrin-A2* and *ephrin-A3* KO mice; Jeffrey Rothstein for providing GLAST and GLT-1 antibodies; Yi Qin, Ju Lu and David States for critical comments on the manuscript; Shinya Ito for help with spine lifetime analysis; Shibo Li, Zhuojun Guo, Maria Ximena Silveyra, Michael Robinson, Benjamin Abrams, Adam Aharon, James Perna, Rebecca Roberts, Andrew Perlik and Jonathan Zweig for suggestions and assistance with experiments. This work was supported by grants from the National Institute of Mental Health to Y.Z.

REFERENCES

- Aoto J, Chen L. Bidirectional ephrin/Eph signaling in synaptic functions. *Brain Res.* 2007; 1184:72–80. [PubMed: 17166489]
- Bock J, Braun K. Blockade of N-methyl-D-aspartate receptor activation suppresses learning-induced synaptic elimination. *Proc Natl Acad Sci U S A.* 1999; 96:2485–2490. [PubMed: 10051669]
- Cahoy JD, Emery B, Kaushal A, Foo LC, Zamanian JL, Christopherson KS, Xing Y, Lubischer JL, Krieg PA, Krupenko SA, et al. A transcriptome database for astrocytes, neurons, and oligodendrocytes: a new resource for understanding brain development and function. *J Neurosci.* 2008; 28:264–278. [PubMed: 18171944]
- Cang J, Kaneko M, Yamada J, Woods G, Stryker MP, Feldheim DA. Ephrin-as guide the formation of functional maps in the visual cortex. *Neuron.* 2005; 48:577–589. [PubMed: 16301175]
- Carmona MA, Murai KK, Wang L, Roberts AJ, Pasquale EB. Glial ephrin-A3 regulates hippocampal dendritic spine morphology and glutamate transport. *Proceedings of the National Academy of Sciences of the United States of America.* 2009; 106:12524–12529. [PubMed: 19592509]

- Changeux JP, Danchin A. Selective stabilisation of developing synapses as a mechanism for the specification of neuronal networks. *Nature*. 1976; 264:705–712. [PubMed: 189195]
- Chaudhry FA, Lehre KP, van Lookeren Campagne M, Ottersen OP, Danbolt NC, Storm-Mathisen J. Glutamate transporters in glial plasma membranes: highly differentiated localizations revealed by quantitative ultrastructural immunocytochemistry. *Neuron*. 1995; 15:711–720. [PubMed: 7546749]
- Choi S, Klingauf J, Tsien RW. Postfusional regulation of cleft glutamate concentration during LTP at 'silent synapses'. *Nature neuroscience*. 2000; 3:330–336.
- Cutforth T, Moring L, Mendelsohn M, Nemes A, Shah NM, Kim MM, Frisen J, Axel R. Axonal ephrin-As and odorant receptors: coordinate determination of the olfactory sensory map. *Cell*. 2003; 114:311–322. [PubMed: 12914696]
- Davy A, Gale NW, Murray EW, Klinghoffer RA, Soriano P, Feuerstein C, Robbins SM. Compartmentalized signaling by GPI-anchored ephrin-A5 requires the Fyn tyrosine kinase to regulate cellular adhesion. *Genes & development*. 1999; 13:3125–3135. [PubMed: 10601038]
- Feldheim DA, Kim YI, Bergemann AD, Frisen J, Barbacid M, Flanagan JG. Genetic analysis of ephrin-A2 and ephrin-A5 shows their requirement in multiple aspects of retinocollicular mapping. *Neuron*. 2000; 25:563–574. [PubMed: 10774725]
- Feng G, Mellor RH, Bernstein M, Keller-Peck C, Nguyen QT, Wallace M, Nerbonne JM, Lichtman JW, Sanes JR. Imaging neuronal subsets in transgenic mice expressing multiple spectral variants of GFP. *Neuron*. 2000; 28:41–51. [PubMed: 11086982]
- Filosa A, Paixao S, Honsek SD, Carmona MA, Becker L, Feddersen B, Gaitanos L, Rudhard Y, Schoepfer R, Klopstock T, et al. Neuron-glia communication via EphA4/ephrin-A3 modulates LTP through glial glutamate transport. *Nature neuroscience*. 2009; 12:1285–1292.
- Fu M, Yu X, Lu J, Zuo Y. Repetitive motor learning induces coordinated formation of clustered dendritic spines in vivo. *Nature*. 2012; 483:92–95. [PubMed: 22343892]
- Hertz L, Zielke HR. Astrocytic control of glutamatergic activity: astrocytes as stars of the show. *Trends in neurosciences*. 2004; 27:735–743. [PubMed: 15541514]
- Holtmaat AJ, Trachtenberg JT, Wilbrecht L, Shepherd GM, Zhang X, Knott GW, Svoboda K. Transient and persistent dendritic spines in the neocortex in vivo. *Neuron*. 2005; 45:279–291. [PubMed: 15664179]
- Huai J, Drescher U. An ephrin-A-dependent signaling pathway controls integrin function and is linked to the tyrosine phosphorylation of a 120-kDa protein. *J Biol Chem*. 2001; 276:6689–6694. [PubMed: 11053419]
- Hubel DH, Wiesel TN, LeVay S. Plasticity of ocular dominance columns in monkey striate cortex. *Philosophical transactions of the Royal Society of London*. 1977; 278:377–409. [PubMed: 19791]
- Katz LC, Shatz CJ. Synaptic activity and the construction of cortical circuits. *Science*. 1996; 274:1133–1138. [PubMed: 8895456]
- Klein R. Bidirectional modulation of synaptic functions by Eph/ephrin signaling. *Nature neuroscience*. 2009; 12:15–20.
- Koeberle PD, Bahr M. The upregulation of GLAST-1 is an indirect antiapoptotic mechanism of GDNF and neurturin in the adult CNS. *Cell death and differentiation*. 2008; 15:471–483. [PubMed: 18064044]
- Lai KO, Ip NY. Synapse development and plasticity: roles of ephrin/Eph receptor signaling. *Curr Opin Neurobiol*. 2009; 19:275–283. [PubMed: 19497733]
- Lichtman JW, Colman H. Synapse elimination and indelible memory. *Neuron*. 2000; 25:269–278. [PubMed: 10719884]
- Micheva KD, Busse B, Weiler NC, O'Rourke N, Smith SJ. Single-synapse analysis of a diverse synapse population: proteomic imaging methods and markers. *Neuron*. 2010; 68:639–653. [PubMed: 21092855]
- Micheva KD, Smith SJ. Array tomography: a new tool for imaging the molecular architecture and ultrastructure of neural circuits. *Neuron*. 2007; 55:25–36. [PubMed: 17610815]
- Murai KK, Nguyen LN, Irie F, Yamaguchi Y, Pasquale EB. Control of hippocampal dendritic spine morphology through ephrin-A3/EphA4 signaling. *Nature neuroscience*. 2003; 6:153–160.
- Murai KK, Pasquale EB. Eph receptors, ephrins, and synaptic function. *Neuroscientist*. 2004; 10:304–314. [PubMed: 15271258]

- Nicoll RA, Malenka RC. Expression mechanisms underlying NMDA receptor-dependent long-term potentiation. *Ann N Y Acad Sci.* 1999; 868:515–525. [PubMed: 10414328]
- Nimchinsky EA, Sabatini BL, Svoboda K. Structure and function of dendritic spines. *Annual review of physiology.* 2002; 64:313–353.
- Pfeiffenberger C, Cutforth T, Woods G, Yamada J, Renteria RC, Copenhagen DR, Flanagan JG, Feldheim DA. Ephrin-As and neural activity are required for eye-specific patterning during retinogeniculate mapping. *Nature neuroscience.* 2005; 8:1022–1027.
- Rose EM, Koo JC, Antflick JE, Ahmed SM, Angers S, Hampson DR. Glutamate transporter coupling to Na,K-ATPase. *J Neurosci.* 2009; 29:8143–8155. [PubMed: 19553454]
- Rothstein JD, Dykes-Hoberg M, Pardo CA, Bristol LA, Jin L, Kuncl RW, Kanai Y, Hediger MA, Wang Y, Schielke JP, Welty DF. Knockout of glutamate transporters reveals a major role for astroglial transport in excitotoxicity and clearance of glutamate. *Neuron.* 1996; 16:675–686. [PubMed: 8785064]
- Sawtell NB, Frenkel MY, Philpot BD, Nakazawa K, Tonegawa S, Bear MF. NMDA receptor-dependent ocular dominance plasticity in adult visual cortex. *Neuron.* 2003; 38:977–985. [PubMed: 12818182]
- Segal M. Dendritic spines and long-term plasticity. *Nat Rev Neurosci.* 2005; 6:277–284. [PubMed: 15803159]
- Sin WC, Haas K, Ruthazer ES, Cline HT. Dendrite growth increased by visual activity requires NMDA receptor and Rho GTPases. *Nature.* 2002; 419:475–480. [PubMed: 12368855]
- Tada T, Sheng M. Molecular mechanisms of dendritic spine morphogenesis. *Curr Opin Neurobiol.* 2006; 16:95–101. [PubMed: 16361095]
- Torii M, Hashimoto-Torii K, Levitt P, Rakic P. Integration of neuronal clones in the radial cortical columns by EphA and ephrin-A signalling. *Nature.* 2009; 461:524–528. [PubMed: 19759535]
- Tzingounis AV, Wadiche JI. Glutamate transporters: confining runaway excitation by shaping synaptic transmission. *Nat Rev Neurosci.* 2007; 8:935–947. [PubMed: 17987031]
- Xu T, Yu X, Perlik AJ, Tobin WF, Zweig JA, Tennant K, Jones T, Zuo Y. Rapid formation and selective stabilization of synapses for enduring motor memories. *Nature.* 2009; 462:915–919. [PubMed: 19946267]
- Yang G, Pan F, Gan WB. Stably maintained dendritic spines are associated with lifelong memories. *Nature.* 2009; 462:920–924. [PubMed: 19946265]
- Yuste R, Bonhoeffer T. Morphological changes in dendritic spines associated with long-term synaptic plasticity. *Annual review of neuroscience.* 2001; 24:1071–1089.
- Zimmer G, Kastner B, Weth F, Bolz J. Multiple effects of ephrin-A5 on cortical neurons are mediated by SRC family kinases. *J Neurosci.* 2007; 27:5643–5653. [PubMed: 17522309]
- Zuo Y, Lin A, Chang P, Gan WB. Development of long-term dendritic spine stability in diverse regions of cerebral cortex. *Neuron.* 2005a; 46:181–189. [PubMed: 15848798]
- Zuo Y, Yang G, Kwon E, Gan WB. Long-term sensory deprivation prevents dendritic spine loss in primary somatosensory cortex. *Nature.* 2005b; 436:261–265. [PubMed: 16015331]

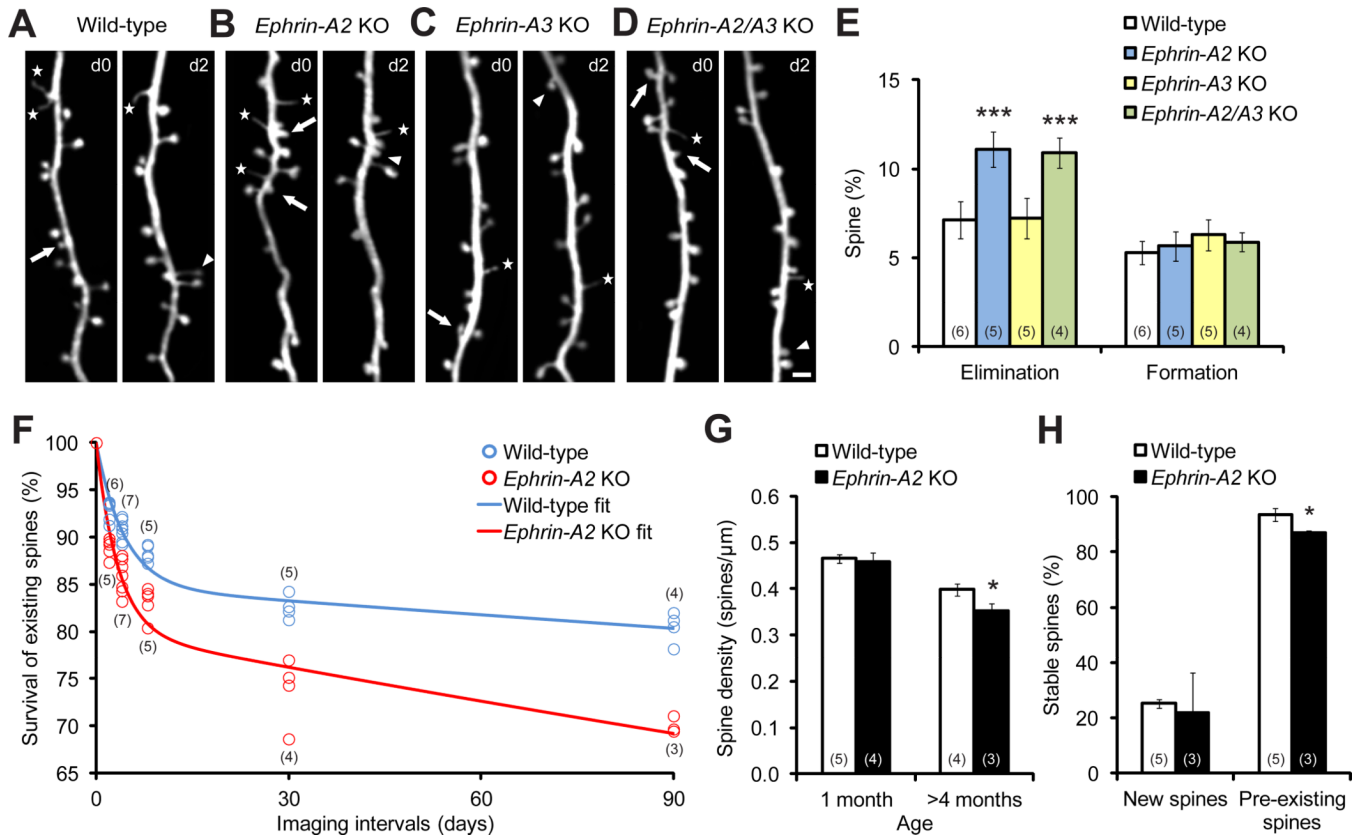


Figure 1. Dendritic Spine Elimination, but not Formation, Is Significantly Increased in One-month-old *Ephrin-A2* KOs

(A–D) Repeated imaging of the same dendritic branches over two-day intervals in the motor cortex reveals spine elimination (arrows) and formation (arrowheads), as well as filopodia (stars), in wild-type (A), *ephrin-A2* KO (B), *ephrin-A3* KO (C) and *ephrin-A2/A3* KO (D) mice. Scale bar, 2 μm .

(E) Percentages of spines eliminated and formed over 2 days in the motor cortex of wild-type and KO mice.

(F) Percentages of spines that survived over 2, 4, 8, 30 and 90 days in wild-type and *ephrin-A2* KO mice. Data were fitted by two-phase exponential decay equations.

(G) Spine density of layer V neuron apical dendrites in wild-type and *ephrin-A2* KO mice in adolescence and adulthood.

(H) Survival percentages of new and pre-existing spines over 4 days in wild-type and *ephrin-A2* KO mice.

Data are presented as mean \pm SD. * $P < 0.05$, *** $P < 0.001$. See also Figures S1 and S2.

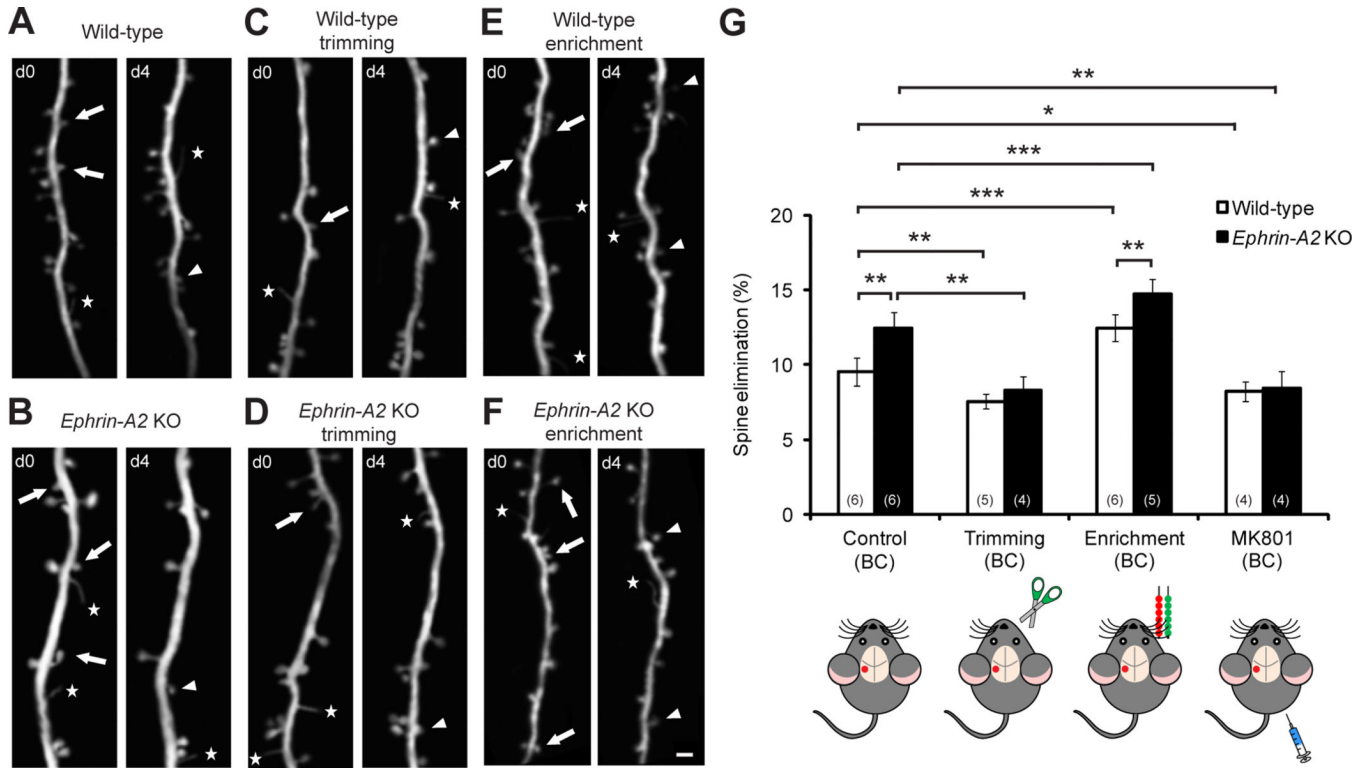


Figure 2. Sensory Experience Is Necessary for Elevated Spine Elimination in *Ephrin-A2* KOs (A–F) Repeated imaging of the same dendritic branches over 4 days in the barrel cortex of wild-type and *ephrin-A2* KO mice under control (A, B), deprived (C, D) and sensory enriched (E, F) conditions. Scale bar, 2 μ m. (G) Percentages of spines eliminated over 4 days in the barrel cortex (BC) under different conditions. Data are presented as mean \pm SD. * P <0.05, ** P <0.01, *** P <0.001. See also Figure S3.

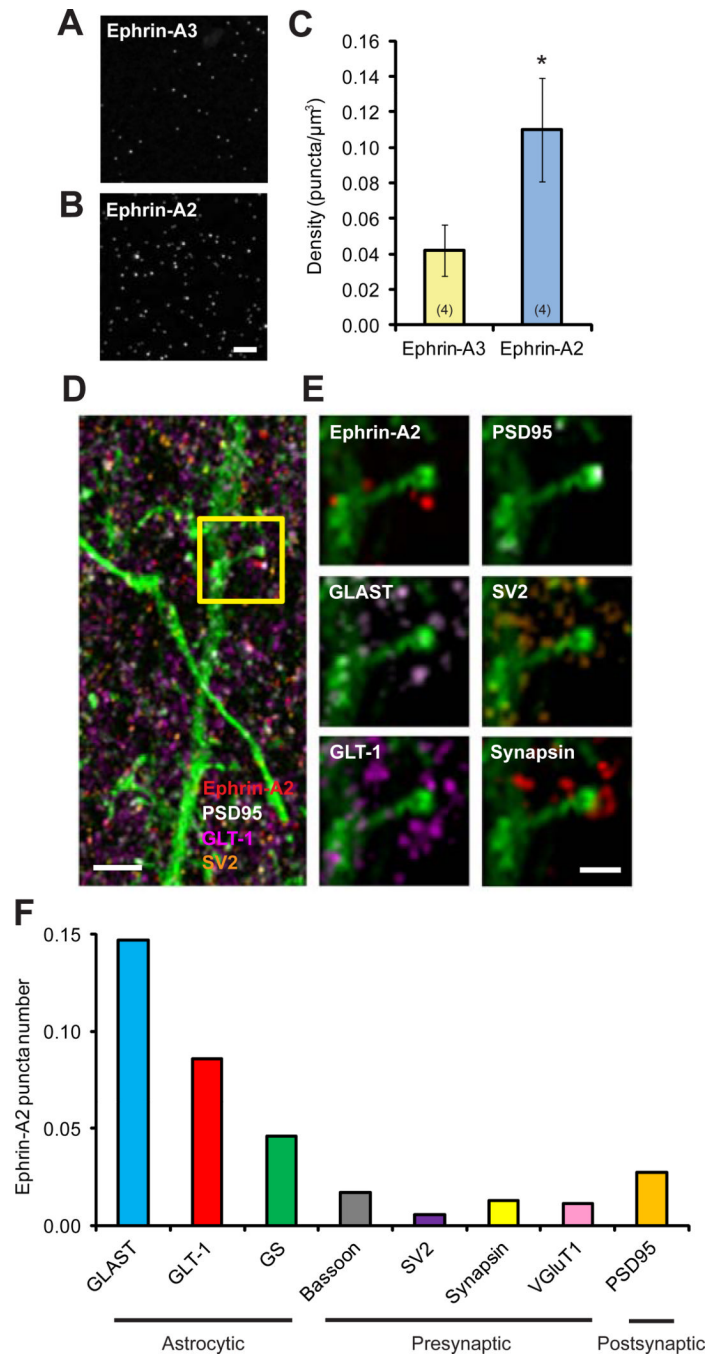


Figure 3. Ephrin-A2 Colocalizes with Astrocytic Glutamate Transporters in the Mouse Cortex

(A, B) Representative image volumes of ephrin-A2 and ephrin-A3 immunofluorescence staining in superficial layer I of one-month-old mouse cortex. Each image is a maximum projection of 5 serial sections. Scale bar, 10 μm . Data are presented as mean \pm SEM.

* $P < 0.05$.

(C) Quantification of puncta density shows that ephrin-A2 is approximately 3 times enriched, compared to ephrin-A3 in the cortex.

(D) Maximum projection of 36 serial sections of ephrin-A2 immunofluorescence (red) with protein markers of presynaptic SV2 (orange), postsynaptic PSD95 (white), astrocytic GLT-1 (magenta) and dendritic segment labeled with YFP (green). Scale bar, 1 μm .

(E) Images of a spine from the boxed region in (D) at higher magnification with various protein markers. Scale bar, 500 nm.

(F) Average numbers of ephrin-A2 puncta within 100 nm from the centers of different neuronal and astrocytic constituents.

See also Figure S4.

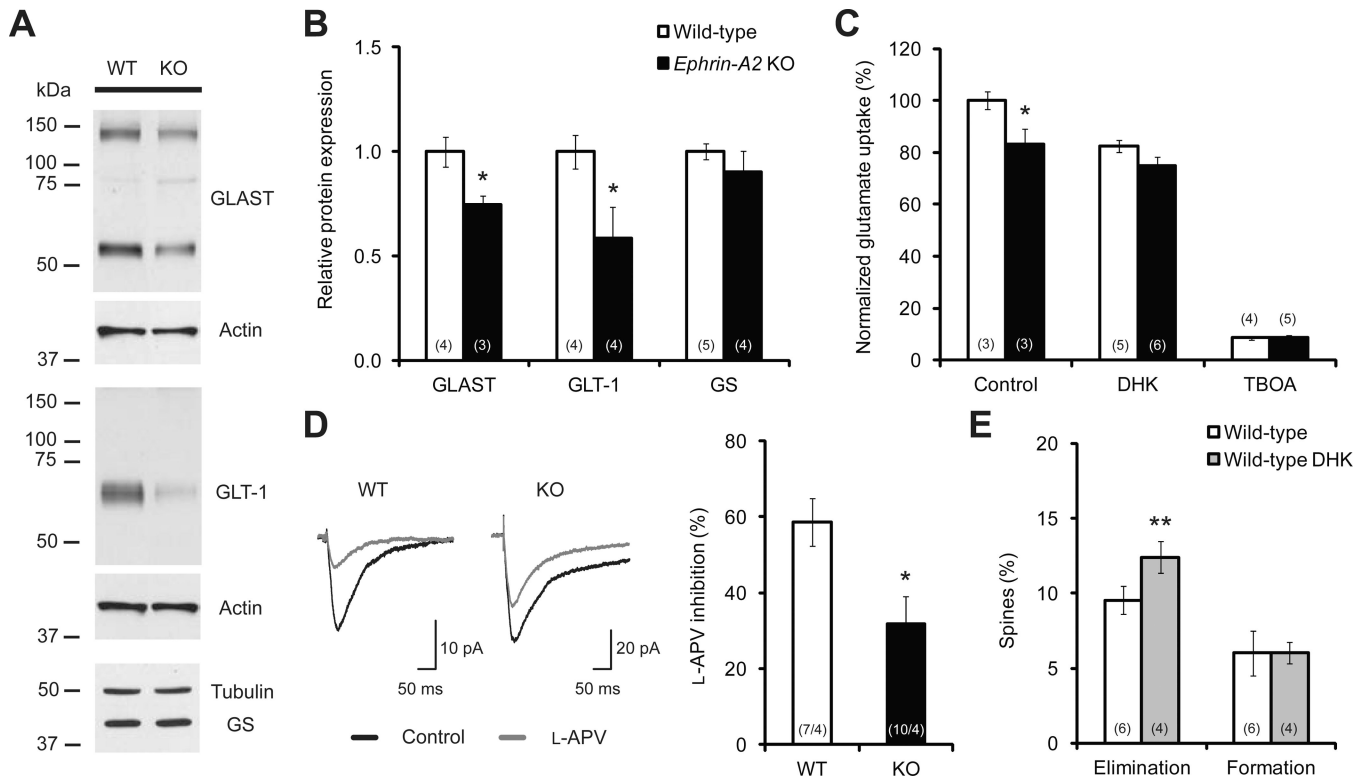


Figure 4. Glial Glutamate Transporters Are Down-regulated in *Ephrin-A2* KOs

(A, B) Western blot examples and quantification reveal a down-regulation of glial glutamate transporters in the cortex of KO mice.

(C) Normalized glutamate uptake efficiencies in cortical slices of one-month-old wild-type and KO mice, with and without glial glutamate transporter inhibitors (DHK and TFB-TBOA).

(D) L-APV inhibition of eEPSCs is significantly reduced in KO cortical slices compared with wild-type slices.

(E) Percentages of spines eliminated over 4 days in wild-type mice with and without DHK treatment.

Data are presented as mean \pm SEM. * P <0.05, ** P <0.01. See also Figure S5.